Dynamical and Observation Models in the Kalman Earth Orientation Filter

T. Mike Chin,* Richard S. Gross,* Dale H. Boggs,* and J. Todd Ratcliff*

The Kalman Earth Orientation Filter (KEOF) developed at the Jet Propulsion Laboratory (JPL) is an operational software system that generates real-time and retrospective estimates as well as predictions of the Universal Time and polar motion (UTPM) parameters used in Earth orientation calibrations to support all JPL interplanetary flight projects. KEOF accomplishes this task by the timely combination of specific UTPM measurements using the Kalman filter and smoother algorithms. The behaviors of KEOF are governed by the stochastic models for the three UTPM parameters as well as the observation models that relate the dynamical variables with the measurements and quantify the measurement uncertainties. Since the first publication of the KEOF's governing equations in 1988, the structures of these stochastic and observation models and their parameter values have undergone steady updates due to advances in scientific understanding of the forces that affect Earth's rotation and orientation as well as improvements in accuracy of the instruments that measure these phenomena. This article describes the past and present versions of stochastic and observation models, including those used currently in KEOF operations. It also suggests potential areas of future improvements.

I. Introduction

The orientation of the Earth with respect to inertial space must be known in order to effectively utilize radiometric data to track and navigate spacecraft. The natural variability in Earth orientation is a significant source of error for high-precision spacecraft tracking and navigation [1]. The Deep Space Network (DSN) thus requires estimates of Earth orientation parameters (EOPs) as a function of time. The Kalman Earth Orientation Filter (KEOF) operation is directed at addressing this requirement.

KEOF provides daily estimates and short-term (up to 80 days) predictions of EOPs. The five traditional components of EOPs are the ecliptic longitude and obliquity offsets of the celestial intermediate pole ($\Delta\psi$ and $\Delta\varepsilon$), x and y components of polar motion (p_X and p_Y), and Universal Time (U). Since the nutation parameters $\Delta\psi$ and $\Delta\varepsilon$ can be modeled to sufficient accuracy, KEOF needs to update and forecast only the Universal Time and polar motion (U, p_X, p_Y), collectively referred to hereafter as UTPM.

* Tracking Systems and Applications Section.

The research described in this publication was carried out by the Jet Propulsion Laboratory, California Institute of Technology, under a contract with the National Aeronautics and Space Administration. Government sponsorship acknowledged.

A 1-milliarcsecond (mas) change in polar motion corresponds to a 3.09-cm translation on Earth's surface (assuming mean Earth radius), while a 1-millisecond (ms) change in Universal Time corresponds to an equatorial displacement of 46.3 cm. The present DSN requirements for Earth orientation estimation errors[1] specify that the error standard deviation (1 sigma) shall be no larger than

- 30 cm in each of the three UTPM components in real time;
- 5 cm in each component for a posteriori reconstructions after 14 days.

The first requirement implies that the UTPM estimates must be updated sequentially in time as soon as new measurements become available, while the second requirement implies that the past UTPM estimates would continue to be updated retrospectively as the measurements are accumulated over time. In the parlance of estimation theory, these procedures are called filtering and smoothing, respectively [2]. Using the Kalman filter algorithm, KEOF generates the UTPM estimates sequentially in time by an optimal combination of heterogeneous EOP measurements. A smoothing algorithm is then used to update the filtered estimates retrospectively based on archived measurements.

The Kalman filter and smoother are based on the Bayesian estimation principle, which requires statistical specifications of the UTPM dynamics and the EOP observation uncertainty in order to determine an optimal solution. To apply the filter algorithm, the UTPM dynamics as well as relations between UTPM and their noisy observations must be expressed in a standard linear dynamic system model [2]. Specifically, the UTPM dynamics are modeled as a vector Markov process

$$\frac{d\mathbf{x}}{dt} = \mathbf{F}\mathbf{x} + \boldsymbol{\omega} \tag{1}$$

where the state vector $\mathbf{x}(t)$ contains the three UTPM variables as well as several auxiliary variables to be described in this article, $\boldsymbol{\omega}(t)$ is a vector of white noise processes [2], and the matrix $\mathbf{F}$ specifies the modeled dynamics. The white noise processes in $\boldsymbol{\omega}(t)$ are assumed to have a joint distribution where the random vector $\int_t^{t+\Delta t} \boldsymbol{\omega}(t')dt'$ at any time t and interval $\Delta t > 0$ has a covariance matrix of $\mathbf{Q}\Delta t$ for a given parameter matrix $\mathbf{Q}$. The observation model is generally given as a linear equation

$$\mathbf{z} = \mathbf{H}\mathbf{x} + \boldsymbol{\nu} \tag{2}$$

where $\mathbf{z}(t)$ is the set of observation data at time t, $\boldsymbol{\nu}(t)$ is the measurement error (uncertainty), and $\mathbf{H}(t)$ is the observation operator that relates each observation with a set of state variables. The measurement error $\boldsymbol{\nu}(t)$ is modeled as a white noise vector with a covariance matrix $\mathbf{R}(t)$. The outcomes of the Kalman filter and smoother are determined primarily by the four parameter matrices of the model equations: the system matrix $\mathbf{F}$, the observation matrix $\mathbf{H}$, and the two covariance matrices $\mathbf{Q}$ and $\mathbf{R}$. The contents and dimensions of the matrices $\mathbf{H}(t)$ and $\mathbf{R}(t)$ are dependent on the number and type of measurements available

[1] *Tracking and Navigation Service: Requirements and Design*, DSMS No. 821-104 Rev. B, JPL D-17235 (internal document), Jet Propulsion Laboratory, Pasadena, California, 2003.

at epoch t and are hence time-varying, while $\mathbf{F}$ and $\mathbf{Q}$ are constant matrices. The purpose of this article is to describe the components and parameters of the model equation [Equations (1) and (2)] used operationally in KEOF.

Since the first publication of KEOF's governing equations in 1988 [3], the model equations and their parameter values have been updated periodically, due to advances in measurement techniques and instrumentations and in scientific understanding of the driving forces for Earth's rotation and wobbles. The operational KEOF software systems are chronologically labeled OP-A, OP-B, and OP-C, with the current version being OP-C. The OP-A version was coded for VAX computers using single-precision numerics, while OP-B was also coded for VAX computers but in double-precision numerics. The OP-C is coded for Linux-based computers using double-precision numerics. The main differences among the KEOF versions are primarily due to the observation data sets used and to updates in the stochastic models, as described in this article.

Section II presents the components of the stochastic model Equation (1), while Section III provides details of the observation model Equation (2). Section IV discusses realization of the full state dynamics. Numerical implementations of the Kalman filter and smoother are outlined in Section V. Section VI concludes with a summary, including a list of potential future upgrades.

II. UTPM Dynamics

The Kalman filter and smoother are algorithms to estimate the state variables of the modeled dynamics [Equation (1)]. The mechanics of UTPM are the central components of the state dynamics. The state dynamics also contain stochastic models of the variables whose role is to excite the UTPM dynamics. These variables are called the excitation processes. The state vector $\mathbf{x}$ thus contains the excitation processes as well as the three UTPM variables. This section describes the dynamics of UTPM and excitation processes.

The third and last category of the state variables is called colored noise processes. The colored noise processes are associated with specific instruments or methods for observations and are described in Section III. All variables in the state $\mathbf{x}$ and stochastic forcing $\boldsymbol{\omega}$ vectors are listed in Tables 1 and 2, respectively. A comprehensive summary of the state equations [Equation (1)] is provided in Section IV.

A. Earth Rotation Mechanics

Models of UTPM dynamics are derived based on the principle of conservation of angular momentum as applied to Earth's rotation. Series of linearization and other reasoned approximations are made [4] to obtain the simple forms described here.

The polar motion is represented by a fixed-period oscillator whose amplitude and phase are modulated by the excitation function χ as

$$\mathbf{p} + \frac{i}{\sigma_{cw}} \frac{d\mathbf{p}}{dt} = \chi \tag{3}$$

Table 1. State variables in KEOF. "Label" names are used in Fortran code (e.g., file `comp.tab`). The "OP-" column shows the KEOF version(s) in which the variable is used. Units: d = day, mas = milliarcsecond, ms = millisecond.

Variable	Label	Unit	OP-	Definition
p_X	PMX	mas	A,B,C	Polar motion, x component
p_Y	PMY	mas	A,B,C	Polar motion, y component
μ_1	MU1	mas	A,B,C	Polar motion excitation, random walk for χ_1
μ_2	MU2	mas	A,B,C	Polar motion excitation, random walk for χ_2
S	S	mas	A,B,C	Polar motion excitation, annual periodicity for χ_2
$\dot{S}$	SDOT	mas/d	A,B,C	Time derivative of S
U	UT1	ms	A,B,C	UT1–TAI
L	LOD	ms/d	A	Excess length of day (LOD), defined as $-dU/dt$
A	AAM	ms/d	B,C	Atmospheric angular momenteum (AAM)
μ_A	MUA	ms/d	B,C	Excitation process $\equiv L - A$
μ_{Aa}	MUA	ms/d	A	Colored noise process for the AAM analysis
b	B	ms/d	A,B,C	Constant bias (noise) in the AAM forecast
μ_{Af}	MUF	ms/d	A,B,C	Colored noise process for the AAM forecast
μ_{G0}	MUGRW	ms/d	B,C	Colored noise for GPS LOD, random walk
μ_{G1}	MUGAR1	ms/d	B,C	Colored noise for GPS LOD, AR-1

Table 2. Elements of the white noise vector $\omega(t)$ that excites the KEOF stochastic model. "Label" names are used in Fortran code (e.g., file `init.nml`). "Power spectral density" values form the diagonal of the parameter matrix $\mathbf{Q}$. The "OP-" column shows the KEOF version(s) in which the variable is used.

Variable	Label	Power Spectral Density	OP-	Definition
ω_1	o3	739.21971252567 mas²/d	C	PMX excitation, random walk
ω_2	o3	739.21971252567 mas²/d	C	PMY excitation, random walk
ω_1	o3	246.4065708418891 mas²/d	A,B	PMX excitation, random walk
ω_2	o3	246.4065708418891 mas²/d	A,B	PMY excitation, random walk
ω_S	o6	$4.263518799241 \times 10^{-4}$ mas²/d³	A,B,C	PMY excitation, annual oscillator
ω_A	o8	0.0036 ms²/d³	B,C	AAM excitation
ω_L	o8	0.0036 ms²/d³	A	LOD excitation
$\omega_{\mu A}$	o9	0.0007 ms²/d³	B,C	AAM-residual excitation
ω_{Aa}	o9	0.0007 ms²/d³	A	AAM analysis colored noise
ω_{Af}	o11	0.00258 ms²/d³	A,B,C	AAM forecast colored noise
ω_{G0}	o12	5×10^{-6} ms²/d³	B,C	GPS LOD error, random walk
ω_{G1}	o13	5×10^{-4} ms²/d³	B,C	GPS LOD error, AR-1

where $i \equiv \sqrt{-1}$ is the unit imaginary number, $\sigma_{cw} \equiv \sigma(1 + i/2Q)$ is the complex-valued (damped) frequency of the Chandler wobble, $\mathbf{p} \equiv p_X(t) - ip_Y(t)$ is the polar motion (complex representation), and $\boldsymbol{\chi} \equiv \chi_1(t) + i\chi_2(t)$, where $\chi_1(t)$ and $\chi_2(t)$ are the x and y components, respectively, of the excitation function. By convention, the positive p_Y direction is defined to be along the meridian at 90 deg west longitude, whereas the positive χ_2 direction is taken to be along the meridian at 90 deg east longitude. (Positive p_X and χ_1 are both aligned at 0 deg longitude.) The two Chandler frequency parameters are estimated

from polar motion measurements and can vary slightly depending on the data sets and techniques used to estimate them (e.g.,[5]). The values used in the operational KEOF are $\sigma = 2\pi/T_{cw} = 2\pi/433$ rad per day and $Q = Q_{cw} = 170$, corresponding to an e-folding decay time of 64 yr (Table 3).

Table 3. Parameters of the dynamical model used currently in KEOF (OP-C version). "Label" names are used in Fortran code (e.g., file `init.nml`).

Parameter	Label	Value	Description
T_{cw}	`cwper`	433 d	Chandler wobble period
Q_{cw}	`qf`	170	Chandler wobble quality factor
T_{aw}	`awper`	365.25 d	Annual wobble period
τ_{aw}	`awdamp`	2500 d	Annual wobble damping time constant
τ_F	`tfl`	5 d	AAM LOD forecast uncertainty time constant
τ_G	`tg`	1/0.44 d	GPS LOD uncertainty time constant

Among the components of Earth orientation, Universal Time varies most dramatically and unpredictably from day to day. The dynamics for Universal Time $U(t)$ can be given as

$$\frac{d}{dt}U = -L \tag{4}$$

where $L(t)$ is the excess length of day (LOD) defined as $(\ell - \ell_0)/\ell_0$ with a unit of ms/day, where ℓ is the instantaneous length of day and ℓ_0 is the reference value of 86,400 s. The Universal Time variable U is defined here as UT1–TAI, where UT1 is the standard measure of the angle about the polar axis through which Earth has rotated, and TAI is a uniform reference time given by atomic clocks. Two commonly used reference time series are Temps Atomique International (TAI) and Coordinated Universal Time (UTC). UTC differs from TAI by an integer number of seconds, since it uses a leap second every year or two to compensate for the fact that Earth's rotation rate — and hence, length of day — varies. By design, the Sun crosses the meridian of Greenwich, England, at noon UTC on average. The date of origin is defined so that $U =$ UT1–TAI was 0 on January 1, 1958.

B. Excitation Processes

The forcing terms (χ_1, χ_2, L) of the UTPM mechanics [Equations (3) and (4)] are often called the excitation functions. In KEOF, each excitation function is modeled as a sum of stochastic processes as

$$\chi_1 = \sum_{i=1}^{N_1} \xi_{1,i}, \quad \chi_2 = \sum_{i=1}^{N_2} \xi_{2,i}, \quad L = \sum_{i=1}^{N_3} \xi_{3,i} \tag{5}$$

where $\xi_{j,i}$ is hereafter referred to as an excitation process. The excitation processes defined in KEOF at present are μ_1, μ_2, μ_A, A, L, S, $\dot{S}$, as listed in Table 1. All excitation processes used in KEOF except for S and $\dot{S}$ are random walk (Brownian motion) processes [6]; S and $\dot{S}$ jointly form a stochastic oscillator.

Each excitation function is modeled empirically. In particular, the polar motion excitation function $\chi(t)$ contains periodicities from a variety of sources, including seasonal oscillations in the surface air pressure [7]. Variations in atmospheric pressure drive the polar motion more effectively over the solid land than the sea surface, as the ocean can compensate for the variations by redistributing its mass (the inverted barometer effect). Due to asymmetries in the distribution of continents and oceans, the χ_2 component is more sensitive to variations in the surface air pressure over land than χ_1. Morabito and others [3] have thus modeled χ_2 as a random walk μ_2 plus an annual oscillation S representing the pressure variation, while modeling χ_1 as only a random walk μ_1, or

$$\chi_1 = \mu_1, \ \chi_2 = \mu_2 + S \tag{6}$$

The dynamics of the excitation processes μ_1, μ_2, and S are in turn given as

$$\frac{d}{dt}\mu_1 = \omega_1, \ \frac{d}{dt}\mu_2 = \omega_2, \ \frac{d^2}{dt^2}S + \alpha_1 \frac{d}{dt}S + \alpha_2 S = \omega_S \tag{7}$$

where ω_1, ω_2, and ω_S are white noise processes listed in Table 2, while $\alpha_1 \equiv 2/\tau_{aw}$ and $\alpha_2 \equiv \alpha_1^2/4 + (2\pi/T_{aw})^2$ are constants such that the resonance period of $S(t)$ would be T_{aw} with the dissipation time of τ_{aw}. Values used for T_{aw} and τ_{aw} can be found in Table 3. All KEOF versions so far (OP-A, B, and C) use the polar motion model [Equations (3,6,7)].

Atmospheric circulation is a dominant contributor to short-term variability of Earth orientation. For Universal Time dynamics, the strong correlation between LOD and atmospheric angular momentum (AAM) is well documented [8,9], and the AAM data from weather forecast models are shown to be particularly effective for accurate forecasts of Universal Time [10]. (See also Section III.C.) In the OP-A version of KEOF, the Universal Time excitation function L, or LOD, is modeled as a single random walk process as

$$\frac{d}{dt}L = \omega_L \tag{8}$$

where ω_L is again an element of the white noise vector $\boldsymbol{\omega}(t)$ as given in Table 2. In this model, AAM is considered to be providing a direct observation of LOD as discussed in Section III.C. In the OP-B and C versions, on the other hand, the physical AAM process A is explicitly introduced as an excitation process. In the new model, LOD is expanded by two excitation processes as

$$L = A + \mu_A \tag{9}$$

where A is the AAM contribution to LOD and μ_A is the residual LOD process, and each excitation process is a state variable modeled as a random walk as

$$\frac{d}{dt}A = \omega_A, \ \frac{d}{dt}\mu_A = \omega_{\mu_A} \tag{10}$$

where ω_A and ω_{μ_A} are elements of $\boldsymbol{\omega}(t)$ as before (Table 2). In the new model, the AAM data are considered to be providing observations of the state variable A (as opposed to L), while all non-atmospheric components of LOD are lumped into the excitation process μ_A.

C. Stochastic Parameterization

Stochastic dynamics of the excitation processes are determined empirically by fitting autoregressive models to time series obtained from historical UTPM trajectories. To model the stochastic behavior of the UTPM parameters, the effects of physical processes that influence the rotation rate in a deterministic and, hence, predictable manner are first excluded from the observed series. Foremost among the predictable processes are the tides of solid Earth and ocean, whose effects can be evaluated using conventional tidal models [11]. Specifically, the effect of the solid-Earth tides is removed by using the model by Yoder and others [12], while the effect of the ocean tides at the Mf, Mf', and Mm tidal frequencies is removed using the model by Kantha and others [13]. Since the former [12] includes a contribution from the equilibrium ocean tides, the latter [13] is used only to correct for deviations from the equilibrium. At present, effects of solid-Earth and ocean tides are removed from only UT1 and LOD but not polar motion. Additionally, annual and semi-annual signals (determined empirically by sinusoidal fits to past measurements) are removed from UT1, LOD, and AAM (Table 4). All removed signals are added back to the filtered and smoothed estimates to recover full UTPM values.

Table 4. Annual and semi-annual signals removed from the LOD, UT1, and AAM observations before ingestion by the Kalman filter. The removed signal for each observation type is given by $C_{\mathrm{ann}} \cos 2\pi(t - t_0)/T_{\mathrm{ann}} + S_{\mathrm{ann}} \sin 2\pi(t - t_0)/T_{\mathrm{ann}} + C_{\mathrm{semi}} \cos 2\pi(t - t_0)/T_{\mathrm{semi}} + S_{\mathrm{semi}} \sin 2\pi(t - t_0)/T_{\mathrm{semi}}$**, where** T_{ann} **and** T_{semi} **are annual and semi-annual periods in days, respectively, and the unit for the reference day** t_0 **is Julian Day (JD). The unit of the harmonic coefficients is milliseconds. The coefficients for UT1 are computed analytically from the LOD coefficients according to Equation (4). "Label" names are used in Fortran code (e.g., file** `comp.tab`**), which defines the shown values in the file** `season.tab`**.**

Observation	Label	t_0	C_{ann}	S_{ann}	C_{semi}	S_{semi}
LOD	`LOD`	2447527.5	0.2880	0.1704	–0.1433	–0.2569
AAM analysis (A_a)	`AAM`	2447527.5	0.3928	0.2821	–0.0516	–0.1672
AAM forecast (A_f)	`FOR`	2447527.5	0.3471	0.2956	–0.0555	–0.1773

The remaining, stochastic components of the UTPM dynamics can usually be modeled by simple regression formulas, especially over the daily to monthly frequency range of interest to the KEOF operations. The random walk characterization of the LOD and AAM processes [14,9,8] is a well-established example of such formulation. The LOD model can also be refined further by expanding it using several excitation processes, as detailed in [15].

As a demonstration of KEOF stochastic modeling procedure, empirical characterization of the polar motion excitation processes μ_1 and μ_2 are considered. Random walk models are also used for μ_1 and μ_2, which can emulate the characteristic slope of the empirical power spectra from GPS data (solid black curves, Figure 1) over the range of periods from a day to 2 weeks that are of interest to KEOF operations. The GPS data are derived from the daily IGS Final combined series of polar motion and its rate (the latter of which facilitates computation of the excitation series without resorting to numerical differentiation), and it is assumed that the estimation error in the GPS data does not contribute significantly to the

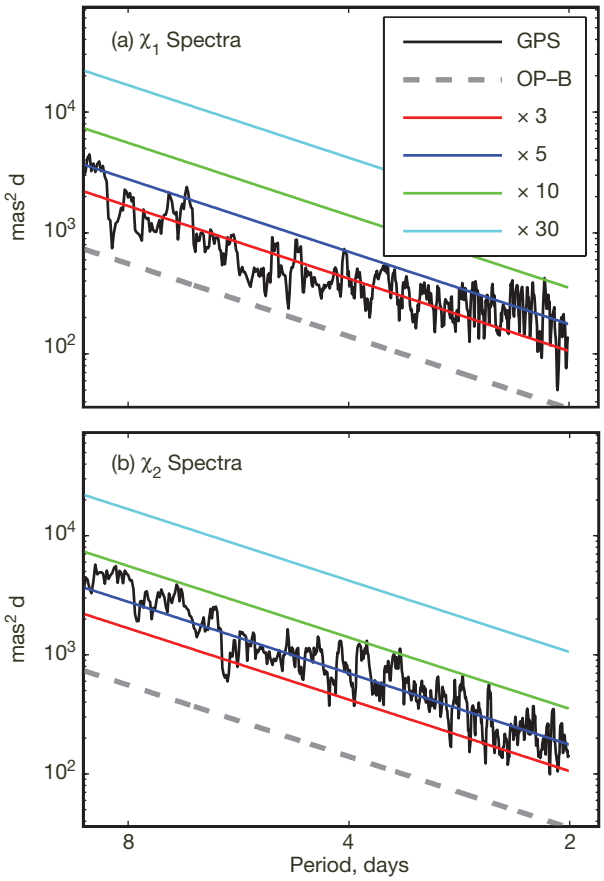

Figure 1. PSDs of polar motion excitations χ_1 and χ_2 computed from IGS Final analyses of polar motion and polar motion rate (solid black curve) and theoretical PSDs of the μ_1 and μ_2 random walk models used in OP-B (gray dashed). Several other random walk PSDs are obtained for each of μ_1 and μ_2 by varying the strength of the forcing white noise processes (ω_1 and ω_2, respectively) controlled by the parameter ○3. Shown are the PSDs obtained when the ○3 parameter value used in OP-B (Table 2) is increased by threefold (red), fivefold (dark blue), tenfold (green), and thirtyfold (light blue).

spectra shown in Figure 1. As EOP measurement accuracy improves over time, occasional updating of KEOF's stochastic parameterizations such as the excitation processes becomes necessary. In particular, the power spectral density (PSD) values (Table 2) of the forcing processes ω_1 and ω_2 used in the OP-B version have been found to be too small, as evident from comparing the spectra of the OP-B random walk models (dashed lines, Figure 1) against the spectra derived from the GPS data. As a result, the power spectra of the OP-B polar motion series (dashed lines, Figure 2) indicate an over-smoothing for the frequencies higher than 60 cycles per year (or periods shorter than 6 days). Since increasing the PSD values of ω_1 and ω_2 by threefold (red lines, Figure 1) would lead to a better match with the GPS data, these new values have been adopted in the current OP-C version (Table 2). The corresponding OP-C polar motion spectra (red lines, Figure 2) show a significant correction of the over-smoothing effects.

Further improvement in parameterization of polar motion excitation is possible. For example, Figure 1(b) indicates that a fivefold, rather than threefold, increase in the PSD values

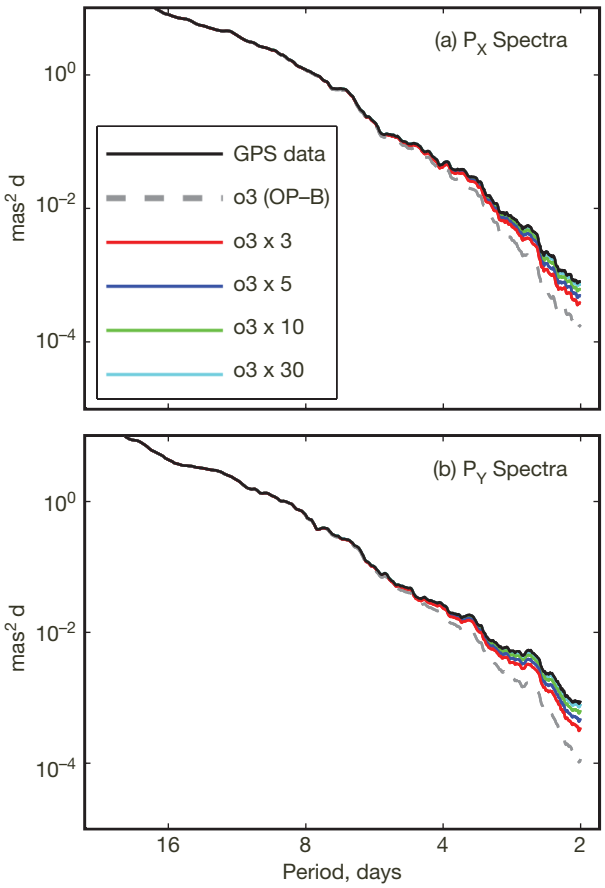

Figure 2. PSDs of the IGS Final polar motion series (solid black curve) and of KEOF polar motion series analyzed using the six o3 parameter values of Figure 1: value used in OP-B (gray dashed), the OP-B value increased by three fold (red), fivefold (dark blue), tenfold (green), and thirtyfold (light blue).

for ω_2 is more consistent with the empirical spectrum. Such additional increase in forcing level of the excitation process μ_2 did not lead to significant change in the polar motion spectra — blue and red curves, Figure 2(b). Modeling of μ_1 and μ_2 should nevertheless reflect asymmetric distribution of land and ocean on Earth's surface, and improved modeling of the polar motion excitation functions is presently under consideration.

D. Improving Stochastic Models of Excitation Processes

The random walk model is used in excitation processes for both UT and PM dynamics. Prediction based on a random walk model implies a persistence of the most recent estimated value. Specifically, for an arbitrary random walk state variable μ, the Kalman filter would use the equation $\frac{d}{dt}\mu = 0$ to generate the prediction. Thus, all future values would be identical to the present estimate, or $\mu(t) = \hat{\mu}(t_p)$ for $t \geq t_p$, where t_p is the time of the most recent data update and $\hat{\mu}$ is the corresponding updated value. Such a prediction scheme based on persistence is particularly problematic because instantaneous effects such as measurement noise could introduce permanent bias in the prediction series.

A remedy for this is to replace the excitation process with a sum $\mu = \bar{\mu} + \lambda$ of a much slower (lower variance) random walk $\bar{\mu}$ and a tapering process λ such as the AR-1 process

$$\frac{d}{dt}\lambda = -\frac{1}{\tau_\lambda}\lambda + \omega_\lambda \tag{11}$$

where ω_λ is white noise and τ_λ is the decay time constant. The role of the slow random walk $\bar{\mu}$ is to capture the long-term trend and mean. Meanwhile, the tapering process λ is designed to respond to short-term changes during the data update operations and to decay smoothly to zero during the forecast operations. The excitation forecast would then reflect the long-term trend or mean as $\mu(t) = \bar{\mu}(t_p)$ without the instantaneous perturbation $\lambda(t) \to 0$ for $t > t_p$.

When a tapering process similar to that described above was used to replace each of the polar motion excitation processes μ_1 and μ_2, polar motion prediction errors were found to decrease by 15 percent for a 10-day lead time and by 20 percent for a 20-day lead time [16]. Also, use of additional annual and semi-annual stochastic oscillators similar to S in Equations (6) and (7) was found to reduce the error by 30 percent for a 10-day lead time and by 50 percent for a 20-day lead time [16]. Such upgrades to the polar motion stochastic models are presently under consideration.

III. Observation Models

KEOF generates UTPM estimates by combining several time-series of independent observations. The observation data include geodetic measurement products from very long baseline interferometry (VLBI), the Global Positioning System (GPS), lunar laser ranging (LLR), and satellite laser ranging (SLR) instruments, as well as analysis and forecast products of AAM from dynamical models used in numerical weather forecasting. Each observation series has a distinct set of physical attributes such as the instrumentation types and analysis/production centers as well as the accuracy, frequency, and latency of reported values. These attributes for the observation series used currently by KEOF are summarized in Table 5.

The observation model [Equation (2)] relates the observed values $\mathbf{z}(t)$ at a given epoch t with the coincident state variables $\mathbf{x}(t)$ and specifies the uncertainty in the observed values as the variances of the additive white noise $\boldsymbol{\nu}(t)$. Most of the observation series report all or part of the three UTPM variables directly. Consequently, the corresponding portions (matrix rows) of the observation operator $\mathbf{H}(t)$ have very simple one-to-one mappings (Section III.A).

There are several exceptions to this simple observation model. First, the UT0 and variation of latitude (VOL) observation series from the single-station LLR and the T and V series from JPL's single-baseline VLBI (see Table 5) report degenerate (singular) linear combinations of UTPM variables. The corresponding rows of the observation matrix $\mathbf{H}(t)$ are non-elementary. Second, the observation models for the AAM and GPS LOD series contain both the standard white noise $\boldsymbol{\nu}(t)$ (which is uncorrelated in time) and time-correlated noise processes. The latter are commonly called colored noise processes. Since correlation structures in the colored noise are modeled by stochastic dynamics, the colored noise processes are members

Table 5. Observations used by KEOF as of January 6, 2009. Each "quantity used" is a distinct measurement series, where PMX and PMY are x and y components of polar motion. Each of the "transverse" (T) and "vertical" (V) components of the Earth orientation, UT0, and variation of latitude (VOL) is a linear combination of PMX, PMY, and UT1 (see text). Listed under "constrained variables" are the state variables from the current KEOF version (OP-C). The "frequency" of each measurement technique is not strictly regular due partly to data drop-outs. For data "latency," a typical value is listed, with the minimum value noted within the parentheses.

Observation Set	Type	Quantities Used	Constrained Variables	Typical Uncertainty*	Frequency	Latency, days
JPL TEMPO	VLBI	T, V	p_X, p_Y, U	0.3, 1.2 mas	Twice monthly	7 (4)
GSFC Intensives	VLBI	UT1	U	0.025 ms	Daily	3 (1)
GSFC Multibaseline	VLBI	PMX, PMY, UT1	p_X, p_Y, U	0.5, 0.5 mas, 0.015 ms	Every 1–3 days	18 (10)
JPL Quick Look	GPS	PMX, PMY, LOD	$p_X, p_Y, A, \mu_A, \mu_{G0}, \mu_{G1}$	0.2, 0.15 mas, 0.01 ms	Daily	1 (1)
IGS Final Combined	GPS	PMX, PMY	p_X, p_Y	0.06, 0.03 mas	Daily	15 (12)
IGS Rapid Combined	GPS	PMX, PMY	p_X, p_Y	0.07, 0.07 mas	Daily	1 (1)
JPL Lunar Laser Ranging	LLR	UT0, VOL	p_X, p_Y, U	0.075 ms, 1.0 mas	Irregular	Variable (n/a)
ILRS Combined	SLR	PMX, PMY	p_X, p_Y	0.2, 0.2 mas	Daily	7 (7)
NMC 0-hr	AAM	AAM analysis (A_a)	A	0.05 ms	Daily	1 (1)
NMC 120-hr	AAM	AAM forecast (A_f)	A, μ_{A_f}, b	0.05 ms	Daily	1 (1)

*Nominal uncertainty values are listed, since with few exceptions they are time-dependent.

of the state vector $\mathbf{x}(t)$. A random walk or first-order autoregression (AR-1) process [6] is typically used to model colored noise dynamics. These models have been determined empirically using procedures applied similarly to model the excitation processes (Section II.C).

In Section III.A, the general features of the observation model [Equation (2)] are presented. The observation operators for the UT0, VOL, T, and V series are then described in Section III.B. Colored noise and other features of the observation models for the AAM series (Section III.C) and GPS LOD and polar motion rate series (Section III.D) are then detailed.

A. General Features

The general form of KEOF's observation model [Equation (2)] is a linear observation function with additive measurement noise. As described previously (Section II.C and Table 4), deterministic time series such as tides and annual harmonics have been removed from each observation series prior to forming the observation vector $\mathbf{z}(t)$. In addition, the constant

and linear trends, referred to as bias and rate, are adjusted for each series to minimize possible inconsistencies among the instrument types due to differences in measurement reference (e.g., [17]). The stated uncertainties of the measurements are also adjusted by multiplicative and/or additive modifications of the covariance matrix. Both the bias-rate corrections and the uncertainty adjustment parameters for all components of a given data set are determined simultaneously in a multivariate approach using maximum likelihood estimation.[2] Finally, the outlying data points are deleted. The details of these preprocessing procedures can be found in [11].

Since the Kalman filter ingests the observations as they become available, not all the measurement series listed in Table 5 are processed simultaneously at any observation epoch t, which typically happens at a daily interval. Thus, the dimensions of $\mathbf{z}(t)$, $\mathbf{H}(t)$, and $\boldsymbol{\nu}(t)$ are accordingly time-dependent. The error variances and covariances (elements of matrix $\mathbf{R}$) are time-varying in general.

Each row of the observation matrix $\mathbf{H}(t)$ is associated with a measurement value available at time t. As shown in Table 5, the majority of the measurement series are observations of polar motion and UT1, each of which can constrain a UTPM state variable (p_X, p_Y, or U) directly. In such a case, the corresponding row of $\mathbf{H}(t)$ is simply an elementary vector (a vector whose entries are all zeros except for a single entry of a 1), where the position of the lone nonzero entry specifies the state variable constrained by the observation.

B. Single-Station LLR and Single-Baseline VLBI

Quantities reported by the single-station LLR and single-baseline VLBI are linear transformations of the UTPM parameters p_X, p_Y, and U. Each of these measurement techniques can provide only two of three components of the transformed UTPM vector. The observation series are thus "degenerate" since they alone cannot specify UTPM uniquely [11]. They can nevertheless constrain linear combinations of the three UTPM parameters.

The observations from the single-station LLR are UT0 and the VOL denoted as $\Delta\phi$. These are linearly related to p_X, p_Y, U as

$$\begin{aligned} \Delta\phi &= p_X \cos\lambda - p_Y \sin\lambda \\ (\mathrm{UT0} - \mathrm{TAI})\cos\phi &= p_X \sin\lambda \sin\phi + p_Y \cos\lambda \sin\phi + U\cos\phi \end{aligned}$$

where (ϕ, λ) are the latitude and longitude of the station, respectively.

From the single-baseline VLBI, a rotation of Earth about an axis parallel to the baseline does not change the relative position of the radio telescopes with respect to the source; hence, this component of Earth's orientation is not determinable from VLBI observations taken from that single baseline. The observables from the single-baseline VLBI are the transverse (T) and vertical (V) components of Earth orientation [11], and the UTPM parameters can be constrained by T and V as

[2] Described in an unpublished manuscript by L. Sung and J. Alan Steppe, "Estimation of Data Uncertainty Adjustment Parameters for Multivariate Earth Rotation Series," 1994.

$$T = -v_y P_X - v_x p_Y + v_z U$$
$$V = \tau_y p_X + \tau_x p_Y - \tau_z U$$

where (v_x, v_y, v_z) and (τ_x, τ_y, τ_z) are basis vectors of the orthonormal transformation determined by the locations of the two VLBI telescopes [11] and are constants.

C. Atmospheric Angular Momentum Observations

The AAM analyses (A_a) and forecasts (A_f) used by KEOF are provided daily by NOAA's National Centers for Environmental Prediction (NCEP) based on measurements and numerical models of atmospheric dynamics. The atmospheric analysis contains information from up-to-date measurements, while the forecast is primarily the result of forward projection of the atmospheric state using the model dynamics. The daily AAM analysis series from NCEP contains 1 day of AAM data, which is given in 6-hr increments, from midnight to midnight. Operationally, KEOF uses only the AAM values given at midnight. The daily AAM forecast series currently contain 7.5 days of AAM forecasts that are given in 12-hr increments. The current KEOF operation uses only the forecast at the 5-day (120-hr) lead time.

1. OP-A implementation. For the OP-A Universal Time dynamics [Equations (4) and (8)], Freedman et al. [10] have modeled the AAM data (A_a and A_f scaled for conversion to a time unit) to be direct observations of LOD (state variable L) and proposed the following observation models:

$$A_a = L + \mu_{A_a} + \nu_{A_a} \tag{12}$$
$$A_f = L + \mu_{A_a} + \mu_{A_f} + b + \nu_{A_f} \tag{13}$$

where ν_{A_a} and ν_{A_f} are the time-uncorrelated components of the measurement uncertainty (whose variance values are given in Table 5) and μ_{A_a}, ν_{A_f}, and b are the correlated components, or colored noise processes. The structures and parameters of the colored noise processes have been determined empirically from archived coincident series of L, A_a, and A_f as

$$\frac{d}{dt}\mu_{A_a} = \omega_{A_a}, \quad \frac{d}{dt}b = 0, \quad \frac{d}{dt}\mu_{A_f} = -\frac{1}{\tau_F}\mu_{A_f} + \omega_{A_f} \tag{14}$$

where the variance values for the white noise forcing processes ω_{A_a} and ω_{A_f} are given in Table 2, while the regression constant τ_F is given in Table 3. The random walk process μ_{A_a} represents the time-correlated portion of the observation noise when AAM is used as an observation of LOD. The constant b and AR-1 process μ_{A_f} are used collectively to model discrepancy between the AAM analysis A_a and forecast A_f series, as simulations of atmospheric circulation are known to "drift" away from measurements due to model imperfection and numerical errors that lead to low-frequency, time-dependent bias. Note that b is technically a random walk whose forcing process happens to have a power of zero. With a nonzero power, b can be used to model a slowly varying drift rather than a constant bias.

2. OP-B and C implementation. In the OP-B and C Universal Time model [Equations (4,9, 10)], LOD L is no longer a state variable but is represented by two excitation processes as $L = A + \mu_A$, where the state variable A represents the physical AAM process (the total

effect of AAM on LOD). This newer representation for L is more consistent with the observation that the spectral power of L is greater than that of A [10]. Since all non-atmospheric components of LOD dynamics are lumped into the state variable μ_A, the AAM data A_a and A_f are now considered to be observations of the variable A (as opposed to L). The observation models for the AAM data A_a and A_f are

$$A_a = A + \nu_{Aa} \tag{15}$$

$$A_f = A + \mu_{Af} + b + \nu_{Af} \tag{16}$$

where the noise processes $(\nu_{Aa}, \nu_{Af}, \mu_{Af}, b)$ are identical to those in the OP-A version (Section III.C).

3. Towards a general AAM observation model. Because of the importance of the AAM data to UT1 forecasts, various improvements to the AAM observation model are under consideration for the operations. In particular, since the 1- to 4-day forecasts of AAM may be of higher quality than the 5-day lead time alone (A_f), it can be expected that using other forecast values would improve UT1 prediction by KEOF. Incorporating a larger number of AAM estimates can also be expected to average out potentially anomalous values and reduce effects of some instantaneous events (e.g., wind bursts) that might be singular in a certain realization (i.e., lead time) of the numerical atmospheric state. A preliminary study[3] has shown the possibilities for as much as a 2-cm improvement in the 5-day UT1 prediction when more AAM forecasts with different lead times are incorporated. To formulate a more flexible framework to assimilate additional AAM series into KEOF estimates, the AAM analysis A_a can be considered as a null lead-time forecast. Thus, both A_a and A_f can be denoted as A_n, where $n = 0, \frac{1}{2}, 1, 1\frac{1}{2}, \cdots, 7\frac{1}{2}$ is the forecast lead day for the 12-hourly NCEP forecasts. Specifically, $A_0 \equiv A_a$ and $A_5 \equiv A_f$. Since correlations among these AAM values are expected to be significant, the cross correlations need to be quantified and taken into account for assimilation of the AAM values at multiple lead times. In particular, covariances among ν_{A_n}, denoting the white noise components of the observation error associated with A_n, would have to be determined for the set of n representing lead times of interest. Relative benefits of assimilating various combinations of the available AAM data can then be examined. Such examination is ongoing at present.

D. GPS Observations

The Global Positioning System can be used to determine LOD, polar motion, and polar motion rate. Of these, polar motion and LOD measurements are used by KEOF at present. The only GPS-based LOD measurement used by KEOF at present is the JPL Rapid Service GPS LOD series (Table 5). Use of other GPS analysis products such as IGS Final LOD series is under consideration for future operations. In addition to LOD, GPS can provide measurement of polar motion and polar motion rate. Use of the polar motion rate measurements is also being considered for future operations.

[3] J. T. Ratcliff, "Improving UT1 Predictions with AAM Forecasts," JPL Interoffice Memorandum (internal document), Jet Propulsion Laboratory, Pasadena, California, February 10, 2006.

1. Colored noise processes. The GPS LOD measurements are corrupted by unmodeled motion of the GPS satellite constellation. Consequently, the GPS-measured LOD values should be considered as proxy measurements of Earth's length of day, since they are not unbiased LOD determinations but include non-negligible time-dependent effects of the motion of the GPS satellite constellation. Thus, before combining the GPS-measured LOD values with other, uncorrupted EOP measurements, the effect of the motion of the satellite constellation on the GPS-measured LOD values must be taken into account.

KEOF does this by using colored noise processes to model these effects, which can be estimated by analyzing the difference between the proxy GPS LOD measurements and uncorrupted determinations of Earth's LOD as given by an independent reference series. At present, the effect of the unmodeled motion of the GPS satellite constellation is modeled[4] as the sum of random walk μ_{G0} and AR-1 μ_{G1} processes. Thus,

$$L_{\mathrm{GPS}} = A + \mu_A + \mu_{G0} + \mu_{G1} + \nu_{\mathrm{GPS}} \tag{17}$$

where L_{GPS} is the proxy LOD measurement from GPS, ν_{GPS} is a white-noise element of $\boldsymbol{\nu}(t)$ with its nominal variance value given in Table 5, and the random walk and AR-1 colored noise processes are given as

$$\frac{d}{dt}\mu_{G0} = \omega_{G0}, \quad \frac{d}{dt}\mu_{G1} = -\frac{1}{\tau_G}\mu_{G1} + \omega_{G1} \tag{18}$$

with ω_{G0} and ω_{G1} defined in Table 2 and τ_G given in Table 3. The GPS LOD data are used operationally only in OP-B and later versions of KEOF, in which LOD is modeled as $L = A + \mu_A$ as discussed in Section II.B.

2. Conversion to UT1-like quantity. While the observation equation [Equation (17)] implies that the LOD measurement from GPS is instantaneous, each reported GPS LOD value $L_{\mathrm{GPS}}(t_{ab})$ is actually an average over a time window $[t_a, t_b]$

$$L_{\mathrm{GPS}}(t_{ab}) = \frac{1}{(t_b - t_a)}\int_{t_a}^{t_b} L(t)dt \approx -\frac{\Delta U(t_a, t_b)}{(t_b - t_a)} \tag{19}$$

where $t_{ab} \in [t_a, t_b]$ is the reported observation epoch and $\Delta U(t_a, t_b) \equiv U(t_b) - U(t_a)$ is the UT1 increment. The GPS LOD data are thus potentially better estimates of the UT1 increment

$$\Delta U(t_a, t_b) = (t_a - t_b) \cdot L_{\mathrm{GPS}}(t_{ab}) \tag{20}$$

than the instantaneous LOD at time t_{ab}. Using such UT1 increments, a UT1-like quantity U' can be evaluated from a sequence of the GPS LOD measurements as

$$U'(t_n) = U(t_0) + \Delta U(t_{0,}t_1) + \Delta U(t_{1,}t_2)\cdots + \Delta U(t_{n-1,}t_n) \tag{21}$$

[4] Empirical derivations by K. Hamdan, "Stochastic Modeling of GPS-Derived LOD," JPL Interoffice Memorandum (internal document), Jet Propulsion Laboratory, Pasadena, California, no date.

where $U(t_0)$ is the most recent available UT1 measurement and $[t_{n-1}, t_n]$ is the time interval associated with the most recent GPS LOD observation. The resulting value of U' can then be assimilated by the Kalman filter as an observation for the state variable U at time t_n. KEOF assimilates only the most recent UT1-like quantity $U'(t_n)$.

To compute $U'(t_n)$, the initial UT1 value $U(t_0)$ must be provided externally, and VLBI is currently the only instrument that can provide such a reference UT1 value. KEOF uses the latest available VLBI measurement (among those listed in Table 5) for this purpose. In general, the starting time t_0 of the GPS sequence does not match with the epoch of the latest UT1 from VLBI. Linear interpolations are hence used to co-locate the GPS and VLBI data in time. Also, the averaging intervals of the GPS measurement can be overlapping (or can have gaps in between), and the actual realization of Equation (20) requires an appropriate scaling to adjust for the overlaps (or gaps). For the JPL Rapid Service GPS LOD series, the optimal length of the averaging interval $t_b - t_a$ has been found to be 36 hr by empirically testing different window widths for overall filter performance.

The evaluation of the UT1-like quantity as above is called the INTELA procedure in KEOF operations. At present, KEOF uses the GPS LOD values both for INTELA and as observations of instantaneous LOD as described previously (Section III.D.1). When the INTELA procedure was incorporated into KEOF, real-time accuracy for the UT1 estimate was found to improve by approximately 33 percent.

3. Polar motion rate. The KEOF software has a general facility to assimilate a rate (time-derivative) measurement as follows: Given the system matrix $\mathbf{F}$, the rate $\dot{\mathbf{x}}$ of the state variables can be expressed as $\mathbf{Fx}$, which can be inserted into the observation model of the form of Equation (2) by replacing $\mathbf{x}$ with $\mathbf{Fx}$. In particular, based on the polar motion portions [(Equations (3,6)] of the system equation, the observation model for the polar motion rates $\dot{p}_X$ and $\dot{p}_Y$ would be

$$\begin{bmatrix} \dot{p}_X \\ \dot{p}_Y \end{bmatrix} = \begin{bmatrix} -\frac{\sigma}{2Q} & \sigma & \frac{\sigma}{2Q} & \sigma & \sigma \\ -\sigma & -\frac{\sigma}{2Q} & \sigma & -\frac{\sigma}{2Q} & -\frac{\sigma}{2Q} \end{bmatrix} \begin{bmatrix} p_X \\ p_Y \\ \mu_1 \\ \mu_2 \\ S \end{bmatrix} + \begin{bmatrix} \nu_{\dot{p}_X} \\ \nu_{\dot{p}_Y} \end{bmatrix} \tag{22}$$

where $\nu_{\dot{p}_X}$ and $\nu_{\dot{p}_Y}$ are white noise processes representing the observation uncertainty. Incorporation of polar motion rate measurements is currently under consideration for KEOF operations.

IV. Realizations of State Dynamics

The state dynamics equation [Equation (1)] plays a central role in Kalman filter and smoother realization. Components of the matrix equations have been described previously in Sections II, III.C, and III.D. Specifically, the state vector $\mathbf{x}(t)$ consists of the three UTPM parameters and the variables of excitation processes and colored noise processes (Table 1). The stochastic nature of the KEOF dynamical model originates solely from the excitation and colored noise processes, which are in turn forced by the white noise processes $\boldsymbol{\omega}(t)$

(Table 2). The purpose of this section is to present a composite picture of KEOF state dynamics equations.

In all the UTPM stochastic models discussed so far, the dynamics of UT and PM are independent from each other. The UT and PM portions are thus presented separately.

A. Universal Time State Dynamics

A key feature of KEOF's UT1 model is the use of AAM as a proxy observation for LOD. This is facilitated by the set of colored noise processes. The combination of these models results in the OP-A version of UT dynamics:

$$\frac{d}{dt}\begin{bmatrix} U \\ L \\ \mu_{Aa} \\ b \\ \mu_{Af} \end{bmatrix} = \begin{bmatrix} 0 & -1 & 0 & 0 & 0 \\ 0 & 0 & 0 & 0 & 0 \\ 0 & 0 & 0 & 0 & 0 \\ 0 & 0 & 0 & 0 & 0 \\ 0 & 0 & 0 & 0 & -\frac{1}{\tau_F} \end{bmatrix} \begin{bmatrix} U \\ L \\ \mu_{Aa} \\ b \\ \mu_{Af} \end{bmatrix} + \begin{bmatrix} 0 \\ \omega_L \\ \omega_{Aa} \\ 0 \\ \omega_{Af} \end{bmatrix} \tag{23}$$

In the OP-B and OP-C versions, the LOD state variable L is replaced by two excitation processes, A and μ_A. In addition, two colored noise processes, μ_{G0} and μ_{G1}, are introduced in the observation model for the GPS-based LOD data:

$$\frac{d}{dt}\begin{bmatrix} U \\ A \\ \mu_A \\ b \\ \mu_{Af} \\ \mu_{G0} \\ \mu_{G1} \end{bmatrix} = \begin{bmatrix} 0 & -1 & -1 & 0 & 0 & 0 & 0 \\ 0 & 0 & 0 & 0 & 0 & 0 & 0 \\ 0 & 0 & 0 & 0 & 0 & 0 & 0 \\ 0 & 0 & 0 & 0 & 0 & 0 & 0 \\ 0 & 0 & 0 & 0 & -\frac{1}{\tau_F} & 0 & 0 \\ 0 & 0 & 0 & 0 & 0 & 0 & 0 \\ 0 & 0 & 0 & 0 & 0 & 0 & -\frac{1}{\tau_G} \end{bmatrix} \begin{bmatrix} U \\ A \\ \mu_A \\ b \\ \mu_{Af} \\ \mu_{G0} \\ \mu_{G1} \end{bmatrix} + \begin{bmatrix} 0 \\ \omega_A \\ \omega_{\mu_A} \\ 0 \\ \omega_{Af} \\ \omega_{G0} \\ \omega_{G1} \end{bmatrix} \tag{24}$$

B. Polar Motion State Dynamics

The polar motion mechanics [Equation (3)] are supported by the dynamics of the three excitation processes μ_1, μ_2, S given by Equations (6) and (7) as

$$\frac{d}{dt}\begin{bmatrix} p_X \\ p_Y \\ \mu_1 \\ \mu_2 \\ S \\ \dot{S} \end{bmatrix} = \begin{bmatrix} -\frac{\sigma}{2Q} & \sigma & \frac{\sigma}{2Q} & \sigma & \sigma & 0 \\ -\sigma & -\frac{\sigma}{2Q} & \sigma & -\frac{\sigma}{2Q} & -\frac{\sigma}{2Q} & 0 \\ 0 & 0 & 0 & 0 & 0 & 0 \\ 0 & 0 & 0 & 0 & 0 & 0 \\ 0 & 0 & 0 & 0 & 0 & 1 \\ 0 & 0 & 0 & 0 & -\alpha_2 & -\alpha_1 \end{bmatrix} \begin{bmatrix} p_X \\ p_Y \\ \mu_1 \\ \mu_2 \\ S \\ \dot{S} \end{bmatrix} + \begin{bmatrix} 0 \\ 0 \\ \omega_1 \\ \omega_2 \\ 0 \\ \omega_S \end{bmatrix} \tag{25}$$

where S requires two state variables (S, $\dot{S}$) because it is a second-order autoregression. This realization is used in all operational KEOF versions (OP-A, OP-B, OP-C).

V. Kalman Filtering and Smoothing

The Kalman filter and smoother produce the optimal state estimates by combining the measurements $\mathbf{z}(t)$ in the observation model [Equation (2)] while constraining the state trajectory $\mathbf{x}(t)$ according to the dynamic model [Equation (1)]. Optimality is in the sense of the following least-squares minimization:

$$\min_{\mathbf{x}(t)} \| \mathbf{x}(t_0) - \mathbf{x}_0 \|^2_{\mathbf{P}_0^{-1}} + \int_{t_0}^{t_p} \| \dot{\mathbf{x}} - \mathbf{F}\mathbf{x} \|^2_{\mathbf{Q}^{-1}} dt + \sum_{t \in \mathcal{T}(t_0, t_p)} \| \mathbf{z} - \mathbf{H}\mathbf{x} \|^2_{\mathbf{R}^{-1}} \tag{26}$$

where $\| \mathbf{v} \|^2_{\mathbf{M}} \equiv \mathbf{v}^T \mathbf{M} \mathbf{v}$ denotes weighted inner product; $\dot{\mathbf{x}}$ denotes the time derivative of $\mathbf{x}$; t_0 and t_p are, respectively, the initial and final times of the analysis; $\mathcal{T}(t_0, t_p)$ is the set of observation epoch time-indices during the analysis; $\mathbf{x}_0$ is the given initial condition for the state dynamics [Equation (1)], and $\mathbf{P}_0$ is the error covariance matrix associated with this initial condition. Note that the last two terms in Equation (26) are derived from the equations of dynamics [Equation (1)] and observation [Equation (2)]. The effect of the initial parameters $(\mathbf{x}_0, \mathbf{P}_0)$ on the optimal estimates tends to diminish as the analysis duration $[t_0, t_p]$ increases due to accumulation of the measurements $\mathbf{z}$.

The state trajectory estimated by the smoother, denoted as $\mathbf{x}_S(t)$, is the minimizing solution to the least-squares problem [Equation (26)] for $t_0 \leq t \leq t_p$. The estimate by the filter, denoted as $\hat{\mathbf{x}}(t)$, equals to the minimizing solution only at the final epoch (present time) t_p, or $\hat{\mathbf{x}}(t_p) = \mathbf{x}_S(t_p)$. The filtered estimate $\hat{\mathbf{x}}(t_p)$, however, can be updated recursively using the Kalman filter algorithm as t_p is increased to extend the analysis duration in response to data accumulating over time. The filter recursion can also be propagated into the future (without incorporation of measurements) to produce optimal predictions for $t > t_p$. Smoothing, on the other hand, requires relatively more computational resources for retrospective analysis and storage of the past measurements or state trajectories. Both the filter and smoother algorithms produce error covariance matrices $\widehat{\mathbf{P}}(t)$ and $\mathbf{P}_S(t)$ that accompany the respective estimates $\hat{\mathbf{x}}(t)$ and $\mathbf{x}_S(t)$. The covariance matrices satisfy $\widehat{\mathbf{P}}(t) - \mathbf{P}_S(t) \geq 0$ (positive semi-definite) for $t_0 \leq t \leq t_p$, indicating that the uncertainty in the filtered estimates is expected to be higher than that of smoothed estimates.

Application of the Kalman filter and smoother algorithms requires discretization of the stochastic differential equation [Equation (1)], mainly by deriving a discrete-time state transition matrix from the system matrix $\mathbf{F}$. The formulas used for the discretization procedure are described first in Section V.A. The Kalman filter recursion is presented next in Section V.B. KEOF uses the Kalman filter recursion to generate two filtered state trajectories — one processed forward in time and the other backward in time. The two trajectories are then combined to form the smoothed estimates, as described in Section V.C.

A. Discretization of the Stochastic Model

Given the present state $\mathbf{x}(t)$, a future state value $\mathbf{x}(t + \Delta t)$ can be computed by integrating the stochastic model [Equation (1)] as

$$\mathbf{x}(t + \Delta t) = \mathbf{\Phi}(\Delta t)\mathbf{x}(t) + \int_t^{t + \Delta t} \mathbf{\Phi}(t + \Delta t - \tau)\boldsymbol{\omega}(\tau) d\tau \tag{27}$$

where $\mathbf{\Phi}$ is the state transition matrix given as

$$\mathbf{\Phi}(\Delta t) = \exp(\mathbf{F} \cdot \Delta t) = \sum_{k=0}^{\infty} \frac{\mathbf{F}^k (\Delta t)^k}{k!} \tag{28}$$

and Δt is the interval of time step. Normally, Δt is the interval between adjacent measurement epochs (for the full set of heterogeneous measurement series) or specified output epochs and does not need to be a constant. For numerical stability, an upper limit for Δt is imposed by the software parameter `maxdt`, which is currently 31 days in the operational KEOF code.

Since the interval Δt can be time-dependent in KEOF, the state transition matrix needs to be computed at run-time. Recall that the stochastic model [Equation (1)] consists of dynamically disjoint equations for the core dynamics of PM and UT as well as the excitation and colored noise processes. Each of these processes has an algebraically closed form (rather than an infinite series) formula to realize (or in one case to approximate, as detailed below) a submatrix portion of the state transition matrix [Equation (28)]. The remainder of this section details these submatrix formulas for the state transition matrix $\mathbf{\Phi}(\Delta t)$.

The submatrix formula for the PM dynamics is by far the most complex. Consider the 6 × 6 system matrix in Equation (25), which is operational at present. The system matrix is partitioned into 2 × 2 submatrices and the corresponding state transition matrix is similarly partitioned; these partitioned 6 × 6 matrices can be written respectively as

$$\begin{bmatrix} \mathbf{A} & \mathbf{B} & \mathbf{C} \\ \mathbf{0} & \mathbf{0} & \mathbf{0} \\ \mathbf{0} & \mathbf{0} & \mathbf{D} \end{bmatrix} \text{ and } \begin{bmatrix} \mathbf{\Phi_A} & \mathbf{\Phi_B} & \mathbf{\Phi_C} \\ \mathbf{0} & \mathbf{I} & \mathbf{0} \\ \mathbf{0} & \mathbf{0} & \mathbf{\Phi_D} \end{bmatrix}$$

where $\mathbf{I}$ is the identity matrix (of implied dimensions). Three of the nontrivial state-transition submatrices can be written in closed forms[5] as:

$$\mathbf{\Phi_A} = e^{-\frac{\sigma}{2Q}\Delta t}\begin{bmatrix} \cos\sigma\Delta t & \sin\sigma\Delta t \\ -\sin\sigma\Delta t & \cos\sigma\Delta t \end{bmatrix}, \mathbf{\Phi_B} = \begin{bmatrix} 1 & 0 \\ 0 & -1 \end{bmatrix} + e^{-\frac{\sigma}{2Q}\Delta t}\begin{bmatrix} -\cos\sigma\Delta t & \sin\sigma\Delta t \\ \sin\sigma\Delta t & \cos\sigma\Delta t \end{bmatrix},$$

$$\mathbf{\Phi_D} = e^{-\frac{\alpha_1}{2}\Delta t}\begin{bmatrix} \cos\Omega_o\Delta t + \frac{\alpha_1}{2\Omega_o}\sin\Omega_o\Delta t & \frac{1}{\Omega_o}\sin\Omega_o\Delta t \\ -\frac{\alpha_2}{\Omega_o}\sin\Omega_o\Delta t & \cos\Omega_o\Delta t - \frac{\alpha_1}{2\Omega_o}\sin\Omega_o\Delta t \end{bmatrix}$$

where $\Omega_o \equiv \left(\alpha_2 - \alpha_1^2/4\right)^{1/2}$ is the resonance frequency of the stochastic oscillator. The submatrix $\mathbf{\Phi_C}$ is approximated[6] as an infinite series derived from Equation (28) as

$$\mathbf{\Phi_C} = \sum_{n=1}^{\infty}\left(\frac{(\Delta t)^n}{n!}\sum_{j=1}^{n}\mathbf{A}^{n-j}\mathbf{C}\mathbf{D}^{j-1}\right) = \begin{bmatrix} S_{11}(\Delta t) & S_{12}(\Delta t) \\ S_{21}(\Delta t) & S_{22}(\Delta t) \end{bmatrix}$$

[5] Derived by D. D. Morabito and collaborators in an unpublished version of [3].

[6] Closed-form formulas are available but are more complex: L. Sung, JPL Interoffice Memorandum 335.2-92.05 (internal document), Jet Propulsion Laboratory, Pasadena, California, 1992.

where each $S_{ij}(\Delta t)$ is a polynomial of Δt. KEOF realizes $\mathbf{\Phi}_C$ using a truncated series by limiting each $S_{ij}(\Delta t)$ to be a 10th-order polynomial. The number of terms (order) in the truncated polynomial expansion can be varied by adjusting the software parameter `ncoef`. The polynomial coefficients are evaluated at run-time by subroutine `coefgen`. The other submatrices of the state transition matrix are computed by subroutine `propagate`.

For the UT dynamics, all the current excitation processes are modeled as random walks. In particular, consider the model given by Equations (4) and (5), where $N_3 = 2$ and the excitation processes are given as $\frac{d}{dt}\xi_{3,i} = \omega_{3,i}$. This stochastic model corresponds to the UT dynamics in the OP-B and C versions and can be written in a matrix form as

$$\frac{d}{dt}\begin{bmatrix} U \\ \xi_{3,1} \\ \xi_{3,2} \end{bmatrix} = \begin{bmatrix} 0 & -1 & -1 \\ 0 & 0 & 0 \\ 0 & 0 & 0 \end{bmatrix}\begin{bmatrix} U \\ \xi_{3,1} \\ \xi_{3,2} \end{bmatrix} + \begin{bmatrix} 0 \\ \omega_{3,1} \\ \omega_{3,2} \end{bmatrix}$$

The corresponding state transition matrix can be obtained easily from Equation (28), since the series terminates (becomes null) after two terms as

$$\mathbf{\Phi}_U(\Delta t) = \mathbf{I} + \begin{bmatrix} 0 & -\Delta t & -\Delta t \\ 0 & 0 & 0 \\ 0 & 0 & 0 \end{bmatrix} = \begin{bmatrix} 1 & -\Delta t & -\Delta t \\ 0 & 1 & 0 \\ 0 & 0 & 1 \end{bmatrix}$$

which serves as another submatrix component.

Each of the excitation and colored noise processes can be written as a simple scalar equation, $\frac{d}{dt}\mu = c\mu + \omega$, where c is a constant (0 for a random walk, $-1/\tau_F$ or $-1/\tau_G$ for the AR-1 processes used in OP-C) and is an element of the system matrix $\mathbf{F}$. The corresponding element for the state transition matrix would be given by Equation (28) as $\mathbf{\Phi}_\mu(\Delta t) = \exp(c\Delta t)$.

B. Filtering Formulas

In the Kalman filter, the state trajectory $\mathbf{x}(t)$ at any given time t is considered to be a random vector governed by a Gaussian distribution whose mean is the optimal trajectory $\hat{\mathbf{x}}(t)$ and covariance matrix is given by $\widehat{\mathbf{P}}(t)$. The Kalman filter is an algorithm to compute the mean $\mathbf{x}(t)$ and covariance $\widehat{\mathbf{P}}(t)$ recursively in time. Each recursive step in the Kalman filter has two components: the prediction stage and the update stage. In the prediction stage, the mean and covariance are stepped forward in time using the dynamical equation [Equation (1)], while in the update stage the mean-covariance pair is updated by the noisy measurements [Equation (2)] using Bayes' rule. At any given time t, the dynamically predicted state value (e.g., UTPM forecasts) is called the prior (or a priori) estimate and is denoted as $\overline{\mathbf{x}}(t)$. The prior estimate is updated by the coincident measurements to yield $\hat{\mathbf{x}}(t)$, which is called the posterior (or a posteriori) estimate. The corresponding prior and posterior covariance matrices are denoted as $\overline{\mathbf{P}}(t)$ and $\widehat{\mathbf{P}}(t)$, respectively.

The primary function of the prediction stage is to forecast the future distribution of the dynamical trajectory based on the stochastic model [Equation (1)], given the initial (present) Gaussian distribution. Using the state transition matrix, this can be achieved through the formulas

$$\overline{\mathbf{x}}(t + \Delta t) = \mathbf{\Phi}(\Delta t)\widehat{\mathbf{x}}(t) \tag{29}$$

$$\overline{\mathbf{P}}(t + \Delta t) = \mathbf{\Phi}(\Delta t)\widehat{\mathbf{P}}(t)\mathbf{\Phi}(\Delta t)^T + \int_0^{\Delta t} \mathbf{\Phi}(\tau)\mathbf{Q}\mathbf{\Phi}(\tau)^T d\tau \tag{30}$$

where $\mathbf{Q}$ is the covariance matrix associated with the random forcing ω as described previously. Currently, $\mathbf{Q}$ is a diagonal matrix whose diagonal terms are constants, given in Table 2. Note that Equation (29) is consistent with Equation (27), since the expectation (mean) of the forcing series ω is assumed to be zero. Operationally, the prediction stage is performed by the subroutine `propagate`, while the integral in Equation (30) is computed by the subroutine `qsetup`.

To initialize the filter recursion, the mean $\widehat{\mathbf{x}}(t_0)$ and covariance $\widehat{\mathbf{P}}(t_0)$ at the starting time t_0 must be provided. In the KEOF code, these initial conditions are passed to the main Kalman filtering routine `filter.f` through the name list `init.nml` as the constants `xapri` and `papri`, obtained from a previous filtering run of earlier data. The current KEOF operation is initialized to January 2, 1998.

The purpose of the update stage is to produce the posterior mean and covariance by combining the prediction and measurement through the observation model [Equation (2)]. The formulas used for the update stage can be derived [2] by applying Bayes' rule to the Gaussian distribution as

$$\widehat{\mathbf{P}} = \left(\overline{\mathbf{P}}^{-1} + \mathbf{H}^T\mathbf{R}^{-1}\mathbf{H}\right)^{-1} \tag{31}$$

$$\widehat{\mathbf{x}} = \overline{\mathbf{x}} + \widehat{\mathbf{P}}\mathbf{H}^T\mathbf{R}^{-1}(\mathbf{z} - \mathbf{H}\overline{\mathbf{x}}) \tag{32}$$

where time t is fixed throughout this stage and hence omitted from the formulas. Since the components of the observation equation [Equation (2)] are not defined unless t is at an observation epoch, the data updates [Equations (31) and (32)] are performed only at observation epochs. At other times, we let $\widehat{\mathbf{P}} = \overline{\mathbf{P}}$ and $\widehat{\mathbf{x}} = \overline{\mathbf{x}}$, which is consistent with Equations (31) and (32) if $R^{-1} = 0$. Conceptually, lack of observation can be considered to be equivalent with having a (fictitious) observation with infinite uncertainty variance, or $R^{-1} = 0$.

C. Smoothing Formulas

The Kalman filter recursion is performed forward in time and the resulting trajectory is saved at specified epochs (e.g., twice daily). To obtain a smoothed estimate of the trajectory, the filtered estimate needs to be retrospectively updated dynamically. The first step to achieve smoothing is to perform a Kalman filter recursion backward in time. In KEOF code, the backward filtering is performed by using a negative Δt in the Kalman filter recursion formulas presented above, except that the interval of the integration in Equation (30) is modified as

$$\overline{\mathbf{P}}(t+\Delta t) = \mathbf{\Phi}(\Delta t)\widehat{\mathbf{P}}(t)\mathbf{\Phi}(\Delta t)^T + \int_{\Delta t}^{0} \mathbf{\Phi}(\tau)\mathbf{Q}\mathbf{\Phi}(\tau)^T d\tau \tag{33}$$

It can be shown (e.g., [2]) that the optimally smoothed trajectory $\mathbf{x}_S(t)$ and its covariance $\mathbf{P}_S(t)$ can be computed by a weighted average of the forward and backward trajectories (using the inverse of the covariance matrices as the weights):

$$\mathbf{P}_S = \left(\widehat{\mathbf{P}}_f^{-1} + \overline{\mathbf{P}}_b^{-1}\right)^{-1} \tag{34}$$

$$\mathbf{x}_S = \mathbf{P}_S\left(\widehat{\mathbf{P}}_f^{-1}\widehat{\mathbf{x}}_f + \overline{\mathbf{P}}_b^{-1}\overline{\mathbf{x}}_b\right) \tag{35}$$

where the subscripts $_f$ and $_b$ denote the results of forward and backward filters, respectively (time t is fixed and hence omitted again for brevity). The main product of KEOF is the smoothed trajectory $\mathbf{x}_S(t)$ and its uncertainty variance series given by the diagonal elements of the covariance matrix $\mathbf{P}_S(t)$.

As mentioned previously, KEOF at present uses the software machinery for the forward filter to perform its backward filtering task. This practice effectively approximates the backward filter in two areas: one of these involves the state transition matrix. In the discrete-time implementation adopted here, the backward state transition matrix should correspond to the inverse of the forward matrix $\mathbf{\Phi}(\Delta t)$ from the same time interval; however, the backward matrix $\mathbf{\Phi}(-\Delta t)$ used in the current realization is not exactly the inverse $\mathbf{\Phi}^{-1}(\Delta t)$ due to the approximations (such as the series truncation for $\mathbf{\Phi}_C$) to numerically realize the state transition matrix. The other area of approximation involves initialization of the backward filter. Since there is no knowledge of the future state (UTPM) values, the corresponding uncertainty variance values should, in principle, be infinite. Since a covariance matrix with infinite variances is numerically degenerate, backward filtering is usually accomplished using an alternate Kalman filter algorithm called an information filter, which propagates the inverse of the covariance matrix instead of the covariance matrix itself [2]. Since KEOF at present does not employ such an algorithm, it instead approximates the initial conditions for the backward filter using an arbitrary state vector and a covariance matrix with very large, but finite, variance values.

Approximations in the backward filter can affect the smoothed estimates as well. The two issues mentioned above, however, can be remedied using the Rauch-Tung-Striebel (RTS) smoother (e.g., [2]), which is an algebraic combination of the information filter algorithm and the formulas of optimal averaging [Equations (34) and (35)]. The RTS smoother ingests the result of the forward Kalman filter and produces optimal smoothed estimates using a single recursion that operates backward in time:

$$\mathbf{\Theta}(t) = \widehat{\mathbf{P}}_f(t-\Delta t)\mathbf{\Phi}^T(\Delta t)\overline{\mathbf{P}}_f^{-1}(t) \tag{36}$$

$$\mathbf{P}_S(t-\Delta t) = \widehat{\mathbf{P}}_f(t-\Delta t) - \mathbf{\Theta}(t)[\overline{\mathbf{P}}_f(t) - \mathbf{P}_S(t)]\mathbf{\Theta}^T(t) \tag{37}$$

$$\mathbf{x}_S(t-\Delta t) = \widehat{\mathbf{x}}_f(t-\Delta t) + \mathbf{\Theta}(t)[\mathbf{x}_S(t) - \overline{\mathbf{x}}_f(t)] \tag{38}$$

where Δt corresponds to the interval of the archived forward filter result. An advantage of the RTS smoothing algorithm is that initialization of the backward recursion is straightfor-

ward; it simply uses the latest forward-filter outputs as $\mathbf{x}_S(t_p) = \hat{\mathbf{x}}_f(t_p)$ and $\mathbf{P}_S(t_p) = \hat{\mathbf{P}}_f(t_p)$, where t_p is the final time (at the end of the forward recursion), and presents no issue with numerical degeneracy. Also, a backward state transition matrix, i.e., $\mathbf{\Phi}^{-1}(\Delta t)$ or $\mathbf{\Phi}(-\Delta t)$, is no longer needed. Recently, an experimental RTS smoother has been implemented for the KEOF system. When compared to the currently operational smoother, the approximations in the operational backward filter have been found to introduce negligible discrepancies between the two UTPM smoothed estimates. The RTS smoother code is under consideration to be included for the operational system due to its streamlined numerics.

VI. Conclusion

The KEOF produces estimates and predictions of Universal Time and polar motion using the Kalman filter and smoother algorithms. The mathematical components of the KEOF formulation — the stochastic models, observation models, and the filter and smoother equations — have been presented. Although the operational product from the OP-C version of KEOF has been consistently meeting the current DSN accuracy requirements,[7] it has been shown that the mathematical components of KEOF can be modified in several ways to improve its performance to meet tighter DSN accuracy requirements expected in the future. Also, a number of organizations, both domestic and international, are producing observations of Earth orientation parameters. Observation accuracy of these parameters, as well as scientific understanding of their dynamics, are steadily improving due to technical advances. It can therefore be expected that periodic upgrades of KEOF components will be needed in order to take advantage of these improvements. The mathematical components of the KEOF software have been categorically partitioned and discussed in this article in order to facilitate future modifications. Possible upgrades suggested by this report include:

- Refinements of the polar motion excitation models, including use of nonidentical random walk models for μ_1 and μ_2 (Section II.C), as well as enhancements with AR-1 models and additional annual/semi-annual periodic components (Section II.D).
- Incorporation of all or part of 1- to 7.5-day lead time AAM forecast data, in addition to the 5-day lead-time data (A_f), using a generalized AAM observation model (Section III.C)
- Incorporation of the GPS-based polar motion rate measurements (Section III.D), as well as additional GPS-based LOD series (Section III.D).
- Use of the Rauch-Tung-Striebel smoother in place of the backward filtering and forward–backward combination procedures (Section V.C).

Acknowledgments

The authors would like to acknowledge J. Alan Steppe for carefully reviewing this article and making numerous suggestions to improve it. They also acknowledge past and present KEOF team members, especially Jean O. Dickey and Marc K. Pestana, whose expertise has been consulted repeatedly during the drafting of this article.

[7] *Tracking and Navigation Service: Requirements and Design*, DSMS No. 821-104 Rev. B, JPL D-17235 (internal document), Jet Propulsion Laboratory, Pasadena, California, 2003.

References

[1] J. A. Estefan and W. M. Folkner, "Sensitivity of Planetary Cruise Navigation to Earth Orientation Calibration Errors," *The Telecommunications and Data Acquisition Progress Report*, vol. 42-123, Jet Propulsion Laboratory, Pasadena, California, pp. 1–29, November 15, 1995. http://tda.jpl.nasa.gov/progress_report/42-123/123E.pdf

[2] A. Gelb, ed., *Applied Optimal Estimation*, MIT Press, Cambridge, Massachusetts, 1974.

[3] D. D. Morabito, T. M. Eubanks, and J. A. Steppe, "Kalman Filtering of Earth Orientation Changes," *The Earth's Rotation and Reference Frames for Geodesy and Geodynamics*, pp. 257–267, Kluwer Academic, Norwell, Massachusetts, 1988.

[4] R. S. Gross, "Earth Rotation Variations — Long Period," *Physical Geodesy*, T. A. Herring, ed., *Treatise on Geophysics*, vol. 3, pp. 239–294, Elsevier, Oxford, England, 2007.

[5] C. R. Wilson and R. O. Vincente, "An Analysis of the Homogeneous ILS Polar Motion Series," *Geophysical Journal International*, Royal Astronomical Society, vol. 62, issue 3, pp. 605–616, September 1980.

[6] A. Papoulis, *Probability, Random Variables, and Stochastic Processes*, McGraw-Hill, New York, 1984.

[7] T. M. Eubanks, "Variations in the Orientation of the Earth," *Contributions of Space Geodesy to Geodynamics: Earth Dynamics, Geodynamic Series*, vol. 24, American Geophysical Union, Washington, D.C., 1993.

[8] J. O. Dickey, S. L. Marcus, J. A. Steppe, and R. Hide, "The Earth's Angular Momentum Budget on Subseasonal Time Scales," *Science*, vol. 255, pp. 321–324, January 17, 1992.

[9] T. M. Eubanks, J. A. Steppe, J. O. Dickey, and P. S. Callahan, "A Spectral Analysis of the Earth's Angular Momentum Budget," *Journal of Geophysical Research*, vol. 90, no. B7, pp. 5385–5404, June 1985.

[10] A. P. Freedman, J. A. Steppe, J. O. Dickey, T. M. Eubanks, and L.-Y. Sung, "The Short-Term Prediction of Universal Time and Length of Day Using Atmospheric Angular Momentum," *Journal of Geophysical Research*, vol. 99, no. B4, pp. 6981–6996, April 10, 1994.

[11] R. S. Gross, T. M. Eubanks, J. A. Steppe, A. P. Freedman, J. O. Dickey, and T. F. Runge, "A Kalman-Filter-Based Approach to Combining Independent Earth-Orientation Series," *Journal of Geodesy*, vol. 72, issue 4, pp. 215–235, April 1998.

[12] C. E. Yoder, J. G. Williams, and M. E. Parke, "Tidal Variations of Earth Rotation," *Journal of Geophysical Research*, vol. 86, pp. 881–891, February 1981.

[13] L. H. Kantha, J. S. Stewart, and S. D. Desai, "Long-Period Lunar Fortnightly and Monthly Ocean Tides," *Journal of Geophysical Research*, vol. 103, issue C6, pp. 12639–12647, 1998.

[14] R. D. Rosen and D. A. Salstein, "Variations in Atmospheric Angular Momentum on Global and Regional Scales and the Length of Day," *Journal of Geophysical Research*, vol. 88, pp. 5451–5470, June 20, 1983.

[15] K. Hamdan and L. Sung, "Stochastic Modeling of Length of Day and Universal Time," *Journal of Geodesy*, vol. 70, issue 6, pp. 307–320, March 1996.

[16] T. M. Chin, R. S. Gross, and J. O. Dickey, "Modeling and Forecast of the Polar Motion Excitation Functions for Short-Term Polar Motion Prediction," *Journal of Geodesy*, vol. 78, issue 6, pp. 343–353, December 2004.

[17] Z. Altamimi, C. Boucher, and P. Willis, "Terrestrial Reference Frame Requirements within GGOS Perspective," *Journal of Geodynamics*, vol. 40, issue 4–5, pp. 363–374, November 2005.